MoS_2 nanosheets grown on nickel chalcogenides: controllable synthesis and electrocatalytic origins for hydrogen evolution reaction in alkaline solution

Electronic Supplementary Information

Anchun Long,‡[a] Wanrong Li,‡[a] Min Zhou,*[a] Weicheng Gao,[a] Bitao Liu,[b] Jumeng Wei,[c] Xiuyun Zhang,*[a] Hongfei Liu,[a] Yongjun Liu, [a] Xianghua Zeng*[a]

[a] College of Physical Science and Technology, and Institute of Optoelectronic Technology, Yangzhou University, Yangzhou 225002, P. R. China

[b] Research Institute for New Materials Technology, Chongqing University of Arts and Sciences, Chongqing 402160, P. R. China

[c] College of Chemistry and Materials Engineering, Anhui Science and Technology University, Bengbu 233100, P. R. China

*Corresponding authors' Email: minzhou@yzu.edu.cn (M. Zhou); xyzhang@yzu.edu.cn (X. Zhang); xhzeng@yzu.edu.cn (X. Zeng).

‡ These authors contributed equally to this work.

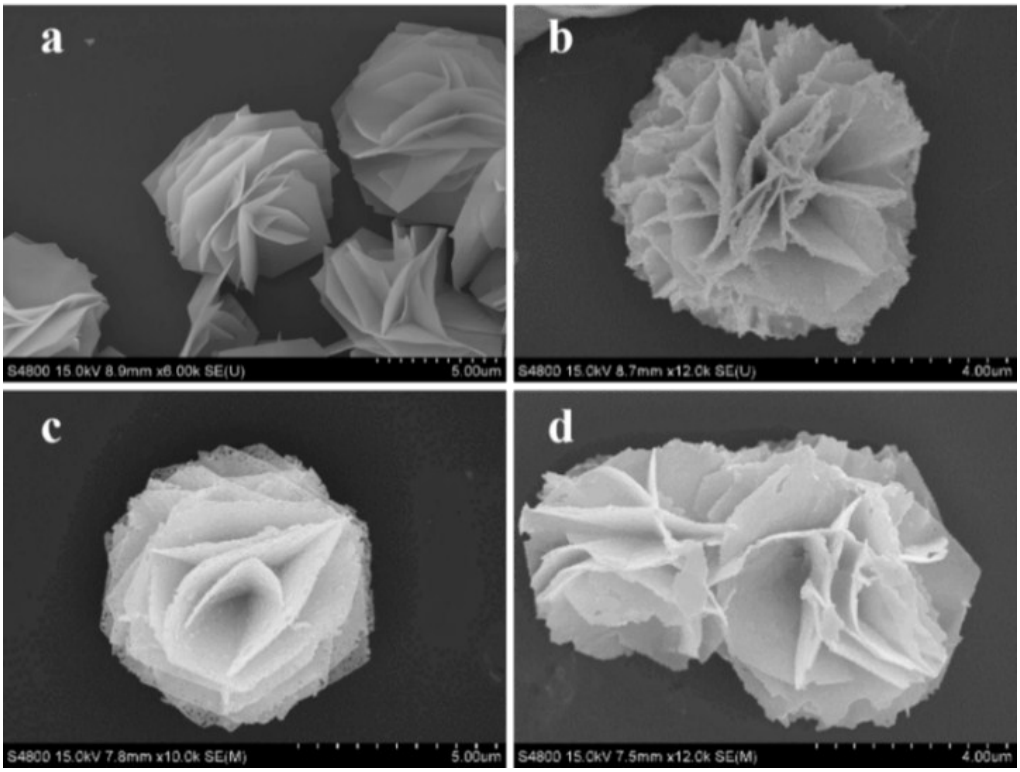

Figure S1. SEM images of $Ni(OH)_2$ precursor (a), NiSe (b), $NiSe_2$ (c), and NiS_2 (d).

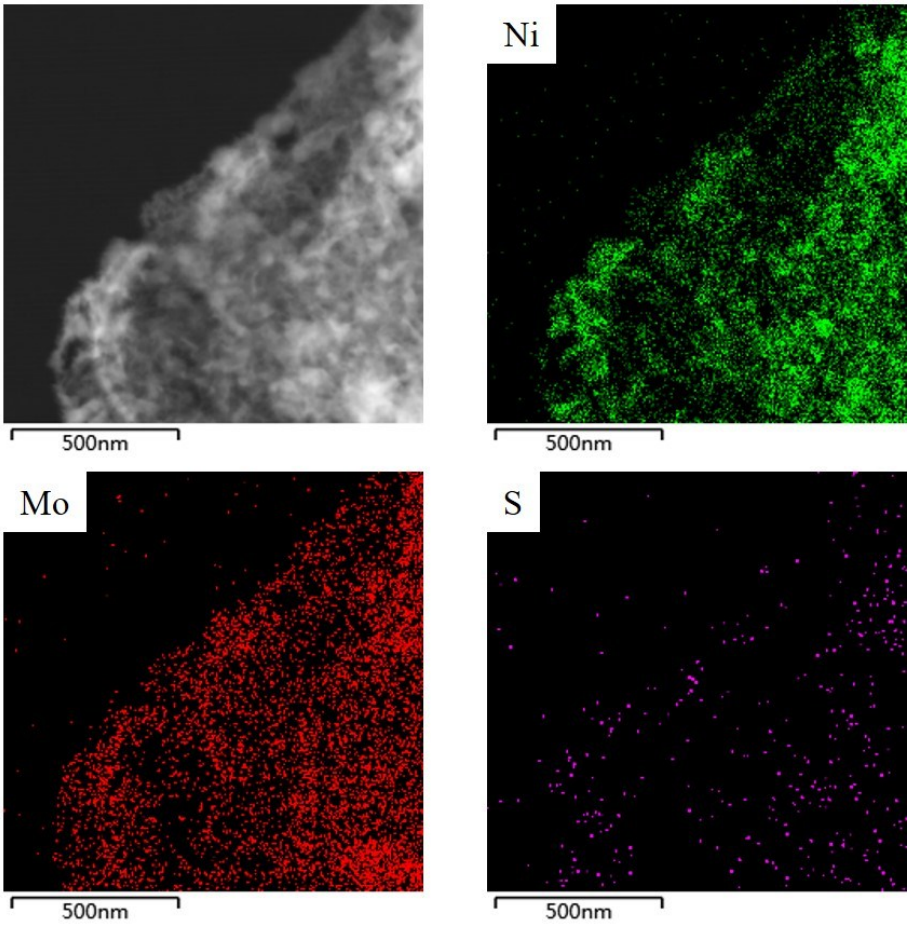

Figure S2. Elemental distribution maps of NiS/MoS_2 heterostructure.

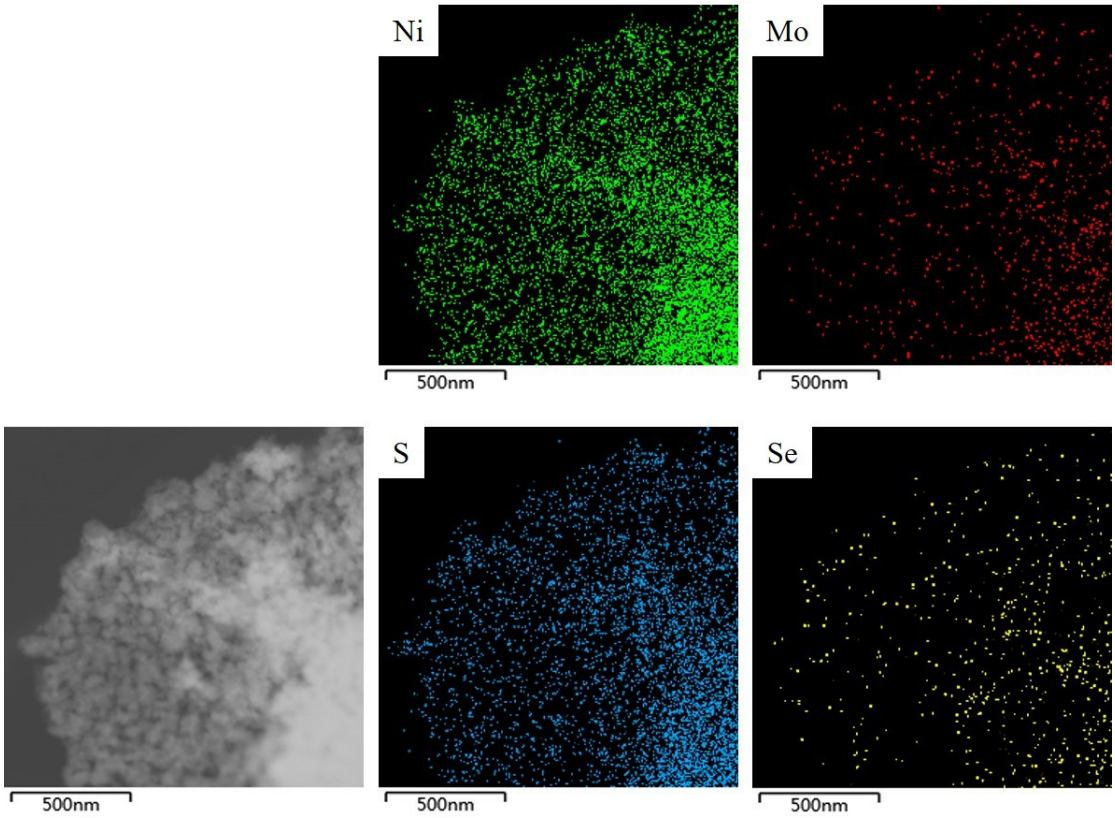

Figure S3. Elemental distribution maps of NiSe/MoS_2 heterostructure.

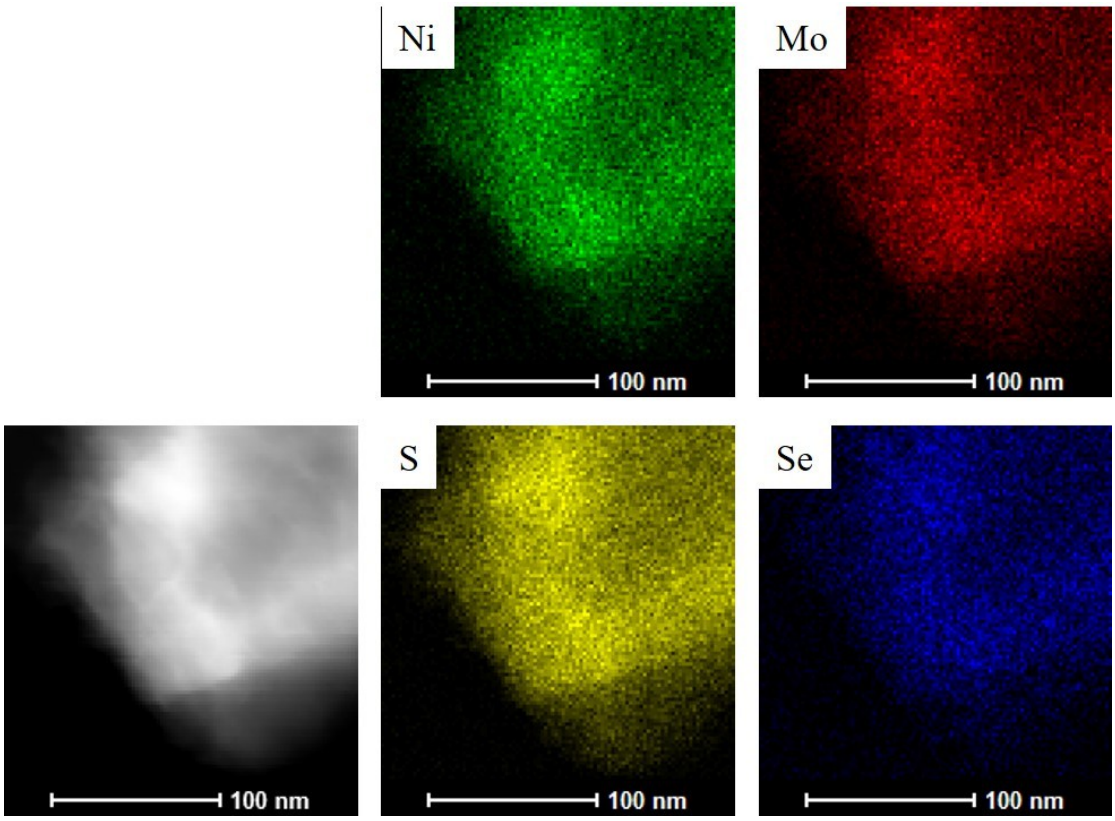

Figure S4. Elemental distribution maps of $NiSe_2/MoS_2$ heterostructure.

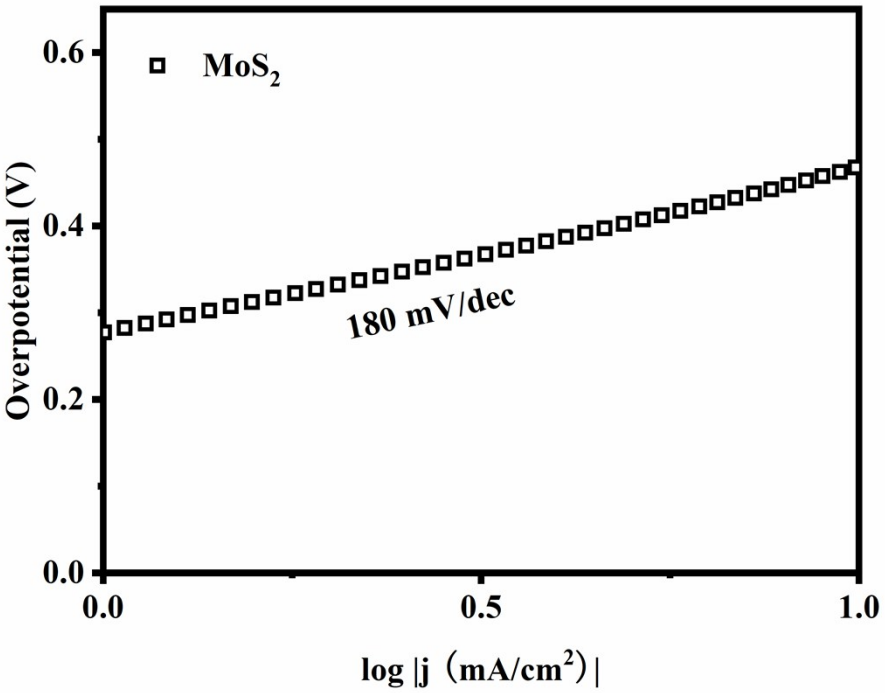

Figure S5. Tafel slope of pristine MoS_2.

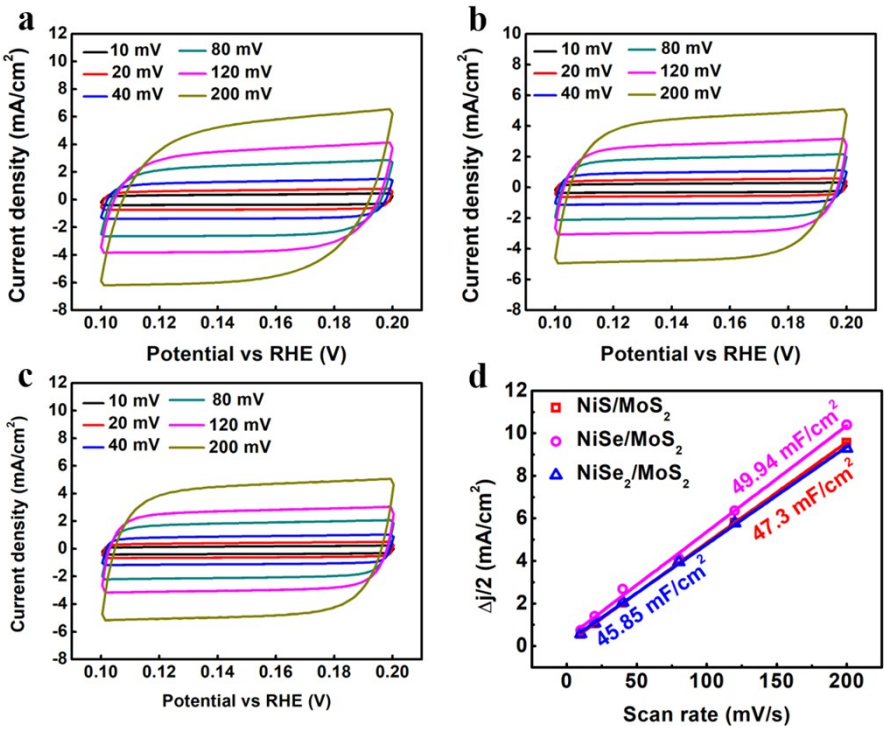

Figure S6. CV curves of NiS/MoS_2 (a), $NiSe/MoS_2$ (b) and $NiSe_2/MoS_2$ (c) at 0.15 V (Vs. RHE) with varied scan rates, and the fitted capacitive current of the three sample (d).

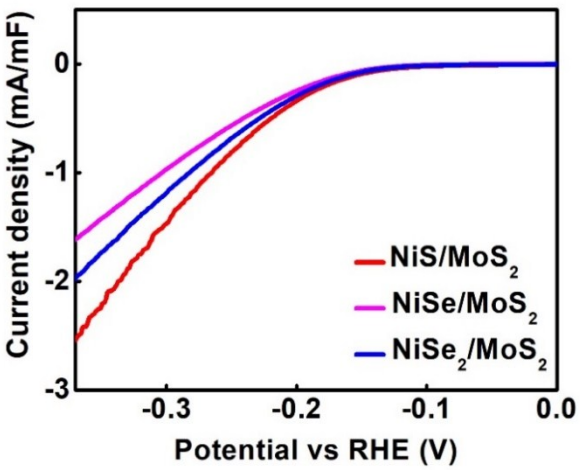

Figure S7. Surface area specified LSV curves of the three heterostructures.

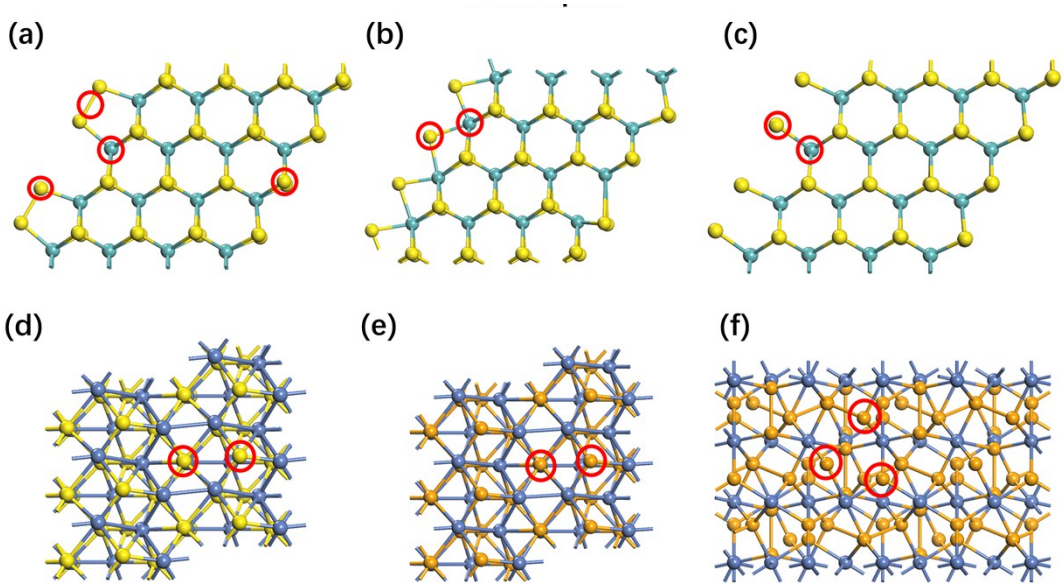

Figure S8. Different proposed positions for H adsorption on (a-c) MoS_2 edge, (d) NiS(101), (e) NiSe(101) and (f) $NiSe_2$(211) facets.

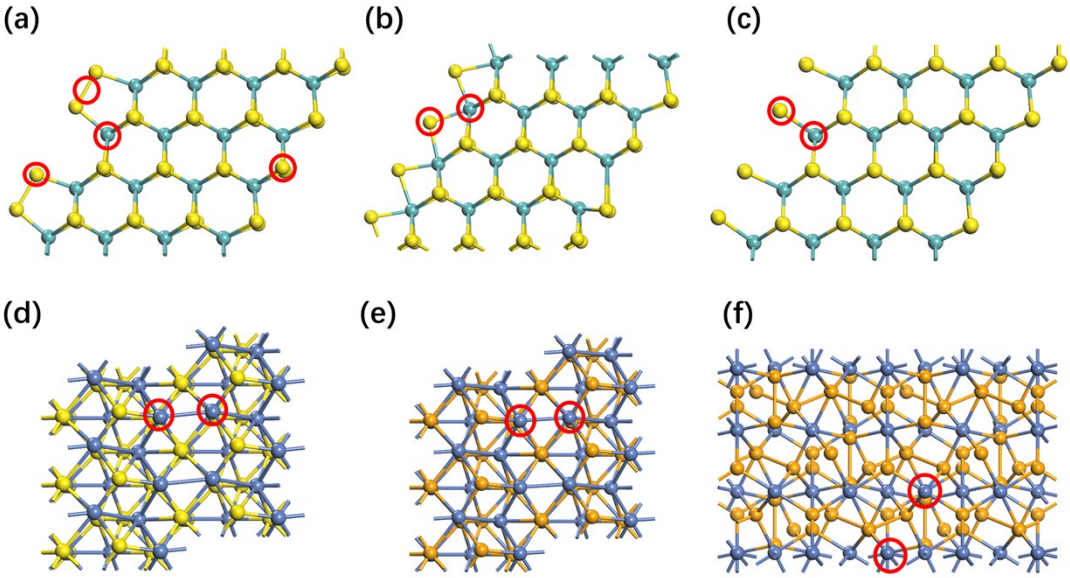

Figure S9. Different proposed positions for OH adsorption on (a-c) MoS_2 edge, (d) NiS(101), (e) NiSe(101) and (f) $NiSe_2$(211) facets.